Evaluation of Electrical Conductivity in Warm Dense Matter of Copper and Gold Generated by Pulsed-Power Discharge with Isochoric Heating

Miki Yasutoshi, Yusuke Amano, Toru Sasaki, Takashi Kikuchi and Nob. Harada

Nagaoka University of Technology, Kamitomioka 1603-1, Nagaoka, 940-2136, Niigata, Japan

ABSTRACT

To evaluate transport properties of warm dense matter (WDM), we have demonstrated an isochoric foam ablation using pulsed-power discharges. We also determined the density dependence of the electrical conductivity for copper and gold at WDM conditions. The measured electrical conductivity of copper agreed with previous experimental results. However the electrical conductivity for gold at the temperature of 3000 K was 10 times larger than the present measurements at 5000 K.

Keywords

Warm Dense Matter, Pulsed-Power, Plasma

1. Introduction

Transport properties of warm dense matter (WDM) are of interest for studies of the interiors of giant planets and for fuel pellets imploded in inertial confinement fusion. The WDM region is referred to densities from 10^{-3} ρ_s (ρ_s is the density of solid matter) to 10 ρ_s and to temperatures ranging from 0.1 eV to 10 eV. To understand the properties of WDM, effects of ion-ion correlations and degenerate electrons are evaluated by studying the dependence of electrical conductivity on density and temperature [1-22]. Several theoretical models exist, such as those of Lee-More-Desjarlais [10], Kuhlbrodt and Redmer [16] and Ichimaru [23]. However the existing experimental data are not sufficient to support or correct these theoretical models. Accurate observations of electrical conductivity in WDM will be required to understand its behavior and the underlying mechanisms.

The purpose of this study is to generate well-defined WDM samples, using pulsed-power discharges, to evaluate the dependence of electrical conductivity on density and temperature.

2.Experimental setup

Figure 1(a) shows the experimental setup. And Figure 1(b) shows an equivalent circuit of experimental setup. The pulsed-power discharge system used to produce WDM by isochoric heating consists of 11.4 μF (6 x 1.9 μF) of capacitor banks, connected by a coaxial electrode to the metal foam enclosed in a sapphire capillary (ϕ 5 mm x 10 mm) [22]. The capacitor bank is charged up to 15 kV to ensure vaporization of the metal foam. Copper and gold samples are used for the experiments. To avoid the skin effect, which

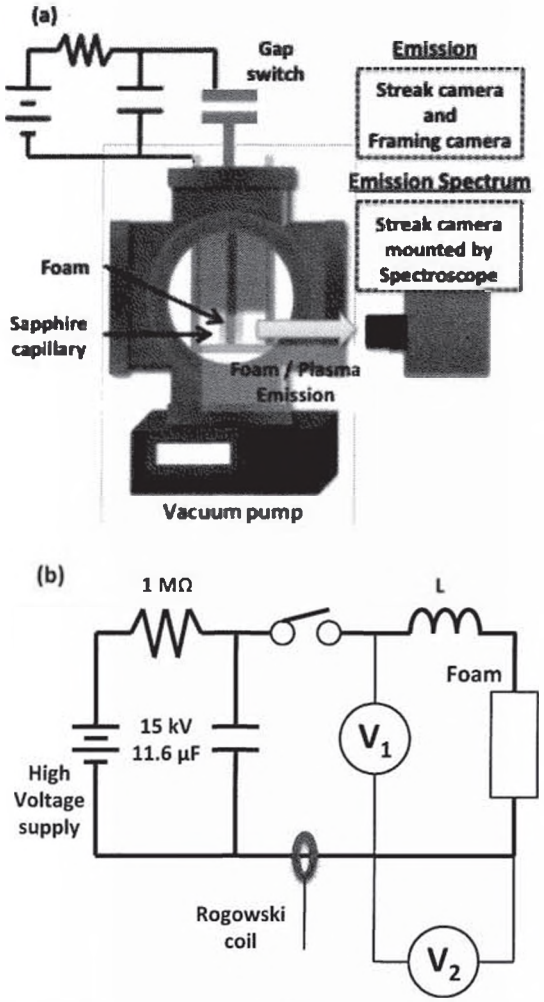

Fig. 1 Experimental setup. (a) Schematic diagram of pulsed-power discharge with isochoric heating. (b) Equivalent circuit

would prevent uniform heating, we use metal foam packed into a sapphire capillary. For the copper foam, the pore size ranges from 50μm to 600μm and the porosity is about 90 %. For gold foam, the numbers are 150 μm and about 84 %, respectively. The time evolution of current $I(t)$ and voltage $V_{foam}(t)$ in foam/plasma are measured with a Rogowski coil and a high-voltage probe (Tektronix : P6015A) [22]. The obtained voltage was composed of resistive and inductive parts. The stray inductance L of the discharge device was estimated to be 165 nH from the preliminary experiment with the short-sircuit. The applied voltage of foam/plasma V_{foam}(t) is estimated to be

□□□□□-□1-□2-□□□□□□ (1)

The electrical conductivity $\sigma(t)$ of the foam/plasma is estimated by

□□=□□□2□(□)□□□□□(□) , (2)

where l is the length and r is the radius of the foam/plasma. To observe the time evolution of the foam/plasma emission, we used a fast framing camera (NAC Imaging Technology: ULTRA Neo) and a streak camera (Hamamatsu Photonics: C7700-1). To evaluate the temperature without use of an equation-of-state model, the emission from the foam/plasma is measured by a spectroscope (Hamamatsu Photonics: C1119-01) mounted on the streak camera [22].

3. Experimental results

3.1 Experimental result of copper

Figure 2 shows typical voltage-current waveforms. We can see that the peak voltage and current are 1.5 kV and 56 kA, respectively. The frequency of these waveforms is estimated to be 83 kHz, i.e., the discharge cycle is 12 μs. The relaxation time from the beginning of ablating foam to the uniform density distribution is a few nsec estimated by the pore size and the sound speed of the metal. Thus, the discharge cycle is much longer than the relaxation time. Thus, the plasma density distribution can be assumed uniform in this timescale.

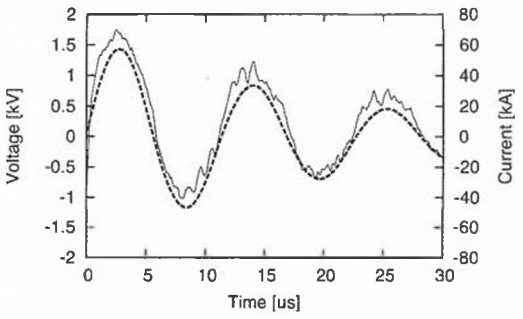

Fig. 2 Typical waveforms of voltage (solid line) and current (dashed line) in 0.1 ρ_s.

Fig. 3 Typical emission of copper foam/plasma

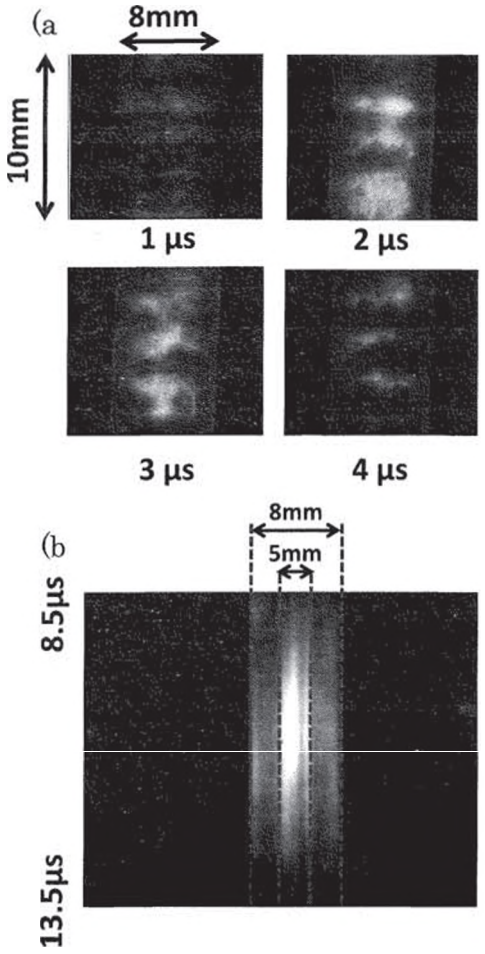

(a) at 1 μs, 2 μs, 3 μs and 4 μs from the beginning of discharge with framing camera (b) from 8.5 μs to 13.5 μs from the beginning of discharge with streak camera.

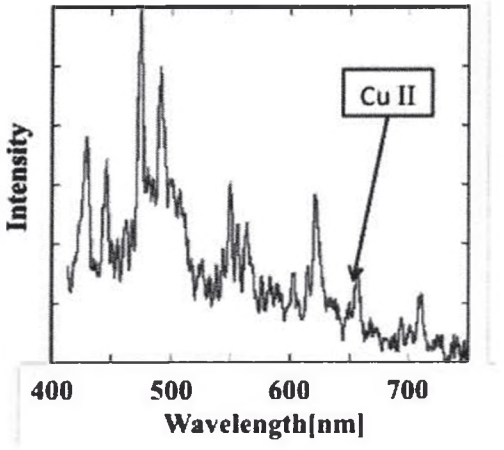

Fig. 4 Typical emission spectrum of copper foam/plasma in $0.1\rho_s$.

Figure 3 (a) shows typical emission at 1 μs, 2 μs, 3 μs and 4 μs from the beginning of discharge observed by framing camera, and (b) shows the typical time-evolution of ablating from 8.5 μs to 13.5 μs observed by streak camera. In these emissions, the expanding of emission is not shown. The results indicated that the foam/plasma can be confined by the sapphire capillary.

Figure 4 shows typical emission spectrum of copper foam/plasma at 12 μs from the beginning of discharge in $0.1\rho_s$. The emission spectrum of Cu II can be confirmed at 651 nm [24].

The foam/plasma temperature T is estimated by the line-pair method. In addition, the foam/plasma temperature is estimated using SESAME equation of state [25] based on the input energy history $E(t)$. The input energy $E(t)$ is expressed as follow:

[illegible] . (3)

The comparison in Figure 5 shows the temperatures determined by these two methods are almost the same. The foam/plasma reaches a temperature over 4000 K at 10 μsec from the beginning of the discharge. Figure 6 shows the time-evolution of the electrical conductivity for the copper foam/plasmas. From these results the electrical conductivity at 4000 K and 0.1 ρ_s is estimated to be of the order of 10^4 S/m.

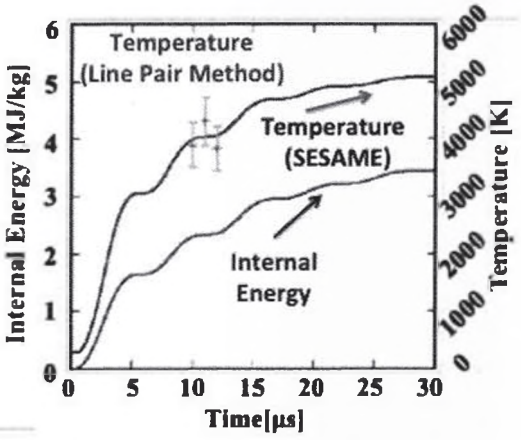

Fig. 5 Typical time evolutions of internal energy and temperature estimated by line-pair method and SESAME equation-of-state table[25]

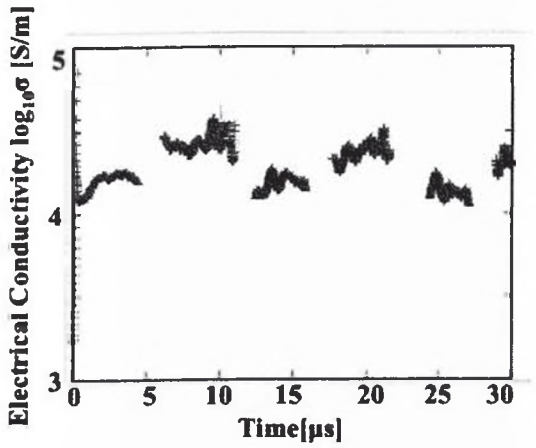

Fig. 6 Typical time evolution of electrical conductivity in $0.1\rho_s$ copper.

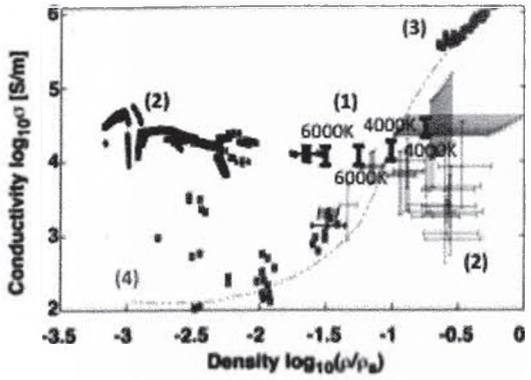

Fig. 7 Electrical conductivity of copper plasma as a function of density, where the point labeled (1) indicates the experimental results obtained in this work (2) indicates the experimental results of Ref. 9 at 5000 K, the point labeled (3) shows the experimental results of Ref. 2 at 6000 K, and the dotted line labeled (4) shows the theoretical prediction of Ref. 10 for 6000 K.

Figure 5 shows the electrical conductivity of copper as a function of density. To compare isochoric heating to other experiments and to the theoretical predictions, typical experimental results (e.g., DaSilva [2] and Sasaki [9]) and theoretical predictions (e.g., Desjarlais [11]) are shown together in Fig.5. The conductivity observed by isochoric heating almost agrees with previous experimental results and theoretical predictions. Additionally, the electrical conductivity of copper obtained by Gathers [28,29] is the order of 10^6 S/m at 4500 K of temperature and $0.7\rho_s$ of density. The electrical conductivity obtained by our experimental results is lower than that obtained by Gathers experiments. It indicated that the conductive electron behaviors might be different in this density dependence. To understand the electron behavior, we will evaluate the electrical conductivity on density region.

3.2 Experimental result of gold

Figure 8 shows typical emission spectrum of gold foam/plasma at 10 μs from the beginning of discharge in $0.11\rho_s$. The emission spectrum of Au II can not be confirmed.

Figure 9 shows typical time evolutions of internal energy and temperature estimated by line-pair method and SESAME equation-of-state table [25] for $0.11\rho_s$ gold. From this result, the foam/plasma reaches a temperature near 3000 K at 10 μsec from the beginning of the discharge.

Figure 10 shows the time-evolution of the electrical conductivity for the gold foam/plasmas in $0.11\rho_s$. From these results the electrical conductivity at 3000 K and $0.11\rho_s$ is estimated to be of the order of 10^4 S/m.

Figure 11 shows the electrical conductivity of gold as a function of density. The isochoric heating experiment described above is compared to previous experiments (e.g., Sasaki [8]) and to theoretical predictions (e.g., Ichimaru [23], L. Spizer [26] and Lee-More [27]). The electrical conductivities of gold at 3000 K are about 10 times higher than the conductivity found in previous experiments (which had a temperature ~ 5000 K).

4. Conclusions

For evaluating the dependence of electrical conductivity on density and temperature, we demonstrated a well-defined WDM source generated by pulsed-power discharges.

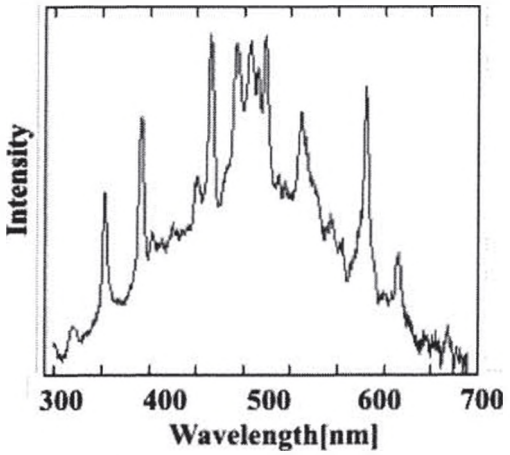

Fig. 8 Typical emission spectrum of gold foam/plasma in $0.1\rho_s$.

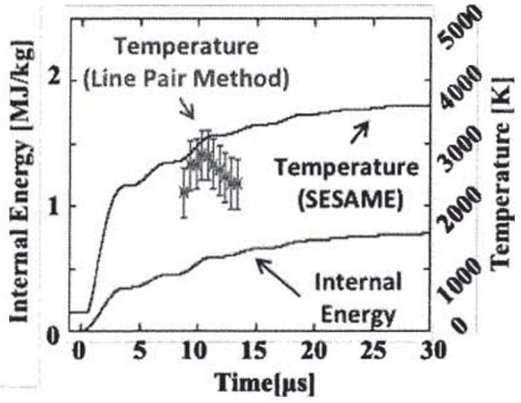

Fig. 9 Typical time evolutions of internal energy and temperature estimated by line-pair method and SESAME equation-of-state table [25] for $0.11\rho_s$ gold.

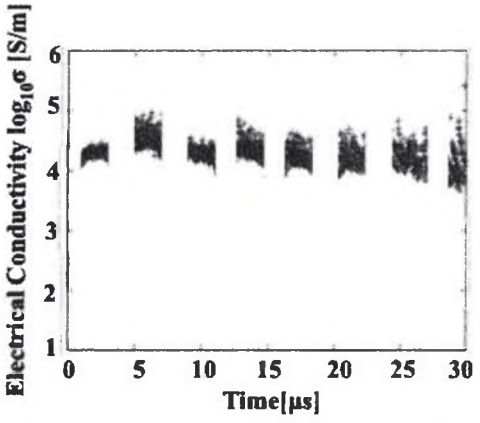

Fig. 10 Typical time evolution of electrical conductivity in $0.11\rho_s$ gold.

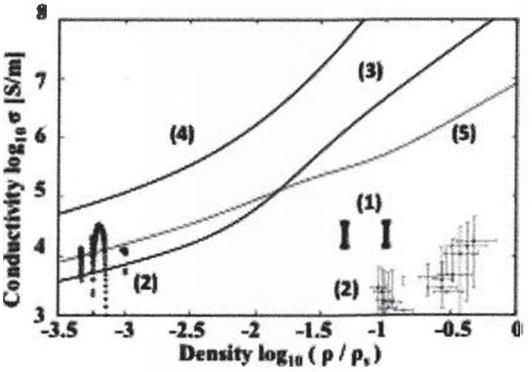

Fig. 11 Electrical conductivity of gold plasma as a function of density, where the point labeled (1) indicates the experimental results obtained in this work for 3000 K (2) indicates the experimental results of Ref. 8 at 5000 K, the line labeled (3) shows the theoretical prediction of Ref. 23 for 5000 K, the line labeled (4) shows the theoretical prediction of Ref. 26 for 5000 K, the line labeled (5) shows the theoretical prediction of Ref. 27 for 5000 K.

Based on the voltage-current waveforms and the optical emission measurements, the metal foam was uniformly heated. The density dependence of electrical conductivity for copper obtained in this work agreed with previous experimental results. However the electrical conductivity for gold at 3000 K in the present work was about 10 times higher than the conductivity at 5000 K in the previous results.

References

[1] R. P. Drake, *High-Energy-Density Physics*, Springer (2006).

[2] A.W. DeSilva and J. D. Katsouros, Phys. Rev. E, **57**, 5945 (1998).

[3] A.W. DeSilva and H. J. Kunze, Phys. Rev. E, **58**, 6557 (1998).

[4] P. Renaudin, C. Blancard, G. Faussurier, and P. Noiret, Phys. Rev. Lett., **88**, 215001 (2002).

[5] H. Yoneda, H. Morikami, K. Ueda,and, and R. M. More, Phys. Rev. Lett., **91**,075004

(2003).

[6] T. Sasaki, Y. Yano, M. Nakajima, T. Kawamura, and K. Horioka, Later Part. Beam, **24**, 371 (2006).

[7] T. Sasaki, Y. Yano, M. Nakajima, T. Kawamura, and K. Horioka, J. Phys.: Conf, Series, **112**, 042027 (2008).

[8] T. Sasaki, Doctor thesis in Tokyo Institute of Technology (2008).

[9] T. Sasaki, M. Nakajima, T. Kawamura, and K. Horikoka, Phys. Plasmas, **17**, 084501(2010).

[10] M. P. Desjarlais, J. D. Kress, and L. A. Colins, Phys. Rev. E, **66**, 025401(2002).

[11] M.P. Desjarlais, Contrub. Plasma Phys., **45**, 73 (2005).

[12] J. Clérouin, P. Renaudin, Y. Laudernet, and P. Noiret, Phys. Rev. B, **73**, 075106 (2006).

[13] M. W. C. Dharma-Wardana, Phys. Rev. E, **73**, 036401 (2006).

[14] [14] S. Mazevet, M. P. Desjarlais, L. A. Collins, J. D. Kress, and N. H. Magee, Phys. Rev. E, **71**, 0164203 (2006).

[15] G. Faussurier, C. Blancard, P. Renaudin, and P. L. Silvestrelli, Phys. Rev. B **73**, 075106 (2006).

[16] R. Redmer, Phys. Rev. E, **59**, 1073 (1999).

[17] S. Kuhlbrodt, and R. Redmer, Phys. Rev. E, **62**, 7191 (2000).

[18] J.J. Barnard, J. Armijo, R.M. More, A. Friedman, I. Kaganovich, B.G. Logan, M.M. Marinak, G.E. Penn, A.B. Sefkow, P. Santhanam, P. Stoltz, S. Veitzer, and J.S. Wurtele, Nuclear Instruments and Methods in Physics Research A, **577**, 275–283 (2007).

[19] P. A. Ni, F. M. Bieniosek, M. Leitner, C. Weber, and W. L. Waldron, Nuclear Instruments and Methods in Physics Research A, **606**, 169–171 (2009).

[20] A. Mancic, J. Robiche, P. Antici, P. Audebert, C. Blancard, P. Combis, F. Dorchies, G. Faussurier, S. Fourmaux, M. Harmand, R. Kodama, L. Lancia, S. Mazevet, M. Nakatsutsumi, O. Peyrusse, V. Recoules, P. Renaudin, R. Shepherd, and J. Fuchs, High Energy Density Physics, **6**, 21–28 (2010).

[21] J. Clérouin, P. Renaudin, Y. Laudernet, and P. Noiret, Phys. Rev. B, **71**, 064203 (2005).

[22] Y. Amano, et. al., Rev. Sci. Instrum., to be published **83**, No. 8 (2012).

[23] H. Kitarura, A. Ichimaru, Phys. Rev. E, **51**, 6004 (1995)

[24] Kramida, A., Ralchenko, Yu., Reader, J. and NIST ASD Team, NIST Atomic Spectra Database (version 5.0), [Online] (2012).

[25] S. P. Lyon, J. D. Johnson, *T-1 Handbook of the SESAME Equation of State Library*, LA-CP-98100 (1998).

[26] L. Spitzer Jr, *Physics of Fully Ionized Gases*, John Wiley and Sons, Inc. (1962)

[27] Y. T. Lee, R. M. More, Phys. Fluids, **27** (1984) 1273.

[28] G. R. Gathers, Int. J. Thermophys., **4**(3), 209-226 (1983)

[29] G. R. Gathers, Rep. Prog. Phys. **49**, 341-396 (1986)